Effect of Micron-scale Photoluminescence Variation on Droop Measurements in InGaN/GaN Quantum Wells

R M Barrett[1], R Ahumada-Lazo[1], J A Alanis[1], P Parkinson[1], S A Church[1], M J Kappers[2], R A Oliver[2] and D J Binks[1]*

[1] Photon Science Institute & Department of Physics and Astronomy, University of Manchester, Manchester, UK

[2] Department of Materials Science & Metallurgy, University of Cambridge, Cambridge, UK

*corresponding author email: david.binks@manchester.ac.uk

Abstract. Micro-photoluminescence maps reveal micron-scale spatial variation in intensity, peak emission energy and bandwidth across InGaN/GaN quantum wells. To investigate the effect of this spatial variation on measurements of the dependence of emission efficiency on carrier density, excitation power-dependent emission was collected from a bright and dark region on each of blue- and green emitting samples. The onset of efficiency droop was found to occur at a greater carrier density in the dark regions than in the bright, by factors of 1.2 and 1.8 in the blue and green-emitting samples, respectively. By spatially integrating the emission from progressively larger areas, it is also shown that collection areas greater than ~50 μm in diameter are required to reduce the intensity variation to less than 10%.

1. Introduction

InGaN/GaN quantum well (QW) structures are widely used as active regions in light emitting diodes (LEDs) for solid-state lighting and large area displays due to the high internal quantum efficiencies attainable at room temperature [1]. However, above an onset value, the internal quantum efficiency decreases with increasing carrier density. Several explanations for this phenomenon, known as 'droop', have been proposed, including: Auger recombination [2], defect-assisted Auger recombination [3], carrier escape [4], and the saturation of localization sites [5]. Distinguishing between these possibilities requires reliable measurements of the carrier densities corresponding to droop onset in QW samples differing in density of both defects and localization sites, the latter varying with In concentration. The onset of droop is typically determined by measuring the spectrally-integrated photoluminescence (PL) intensity as a function of excitation power. Because the excited carrier density needed to obtain droop is high (typically $\sim 10^{12} \text{cm}^{-2}\text{QW}^{-1}$ [6]), a tightly-focussed laser spot with a diameter of a few microns is typically used. Additionally, light should be collected just from the central region of the excitation spot to ensure uniform excitation densities, i.e. well-defined carrier densities [7].

The spatial variation of the emission properties in InGaN/GaN QWs and LEDs has been previously studied using near-field scanning optical microscopy (NSOM) [8,9] and confocal scanning laser microscopy (CSLM) [10–12] in structures emitting across the entire visible spectrum. These reports show that micron and sub-micron scale variations and trends in the emission intensity, wavelength and bandwidth are different depending on the emission energy,

and can be caused by the presence of defects such as V-pits, dislocations and Ga vacancy-impurity complexes. In addition, these variations are also attributed to the combined effects of the band-tail filling of localization sites and the quantum confinement Stark effect (QCSE), depending on indium content and carrier density, all of which can also affect the macroscopic optical properties.

Here, we study the variation of the intensity, peak energy, and bandwidth of PL emission on the micron-scale in the plane of the QWs. We show that if the collection region is too small, this variation can affect the measured excitation power corresponding to the onset of droop such that different values are obtained at different positions on the wafer. We determine the minimum collection spot size such that averaging over the micron-scale variation in PL gives, to within a certain precision, reproducible droop measurements across the sample. This enables meaningful comparisons between samples with different defect densities or In contents.

2. Methods

2.1. Sample growth.
The growth of the samples used in this study was via metal organic chemical vapor deposition (MOCVD) and has been previously reported elsewhere [13] and so is only briefly summarized here. Blue and green emitting InGaN/GaN multiple quantum well (MQW) samples were grown in a 6×2 in. Thomas Swan close-coupled showerhead reactor using trimethylindium (TMI), trimethylgallium (TMG), and ammonia (NH_3) as precursors and nitrogen as the carrier gas; the reactor pressure was 300 Torr. Growth was on GaN pseudo-substrates, which consisted of about 4 μm of GaN on (0001) sapphire substrates. The two temperature (2T) growth method [14] was used, with the QW regions grown at 730 ℃ and 706 ℃ for the blue and green devices, referred to as B730 and G706 from hereon in. The nominal thicknesses of the InGaN QWs and GaN barriers were 3 nm and 7 nm, respectively; 10 and 5 QWs were grown for the blue- and green-emitting samples, respectively. The indium content was estimated to be 10% and 17% for B730 and G706, respectively [14].

2.2. Microphotoluminescence characterization.
The microphotoluminescence (μPL) system used to study the spatial variation in the emission properties of these samples at room temperature has also been previously reported [15]. In brief, the output of a pulsed (∼170 fs pulse duration) Ti:Sapphire (Coherent, RegA 9000) laser source at a repetition rate of 100 kHz was frequency doubled (using a PHOTOP TP-2000B doubler and a 400 nm bandpass filter) to generate a pure excitation wavelength of 400 nm. The spot size at the sample position was measured to be 20 μm after defocusing with an objective lens, however, luminescence was collected from a spot of only 1.5 μm at the centre of the excitation area to ensure that data is collected only from a region of uniform excitation and hence of well-defined carrier densities. The sample was placed on a computer-controlled translation stage allowing the position of the sample relative to the excitation spot to be changed in three dimensions. The position of the sample in the plane of the excitation was changed incrementally in steps of 1.5 μm in both the x and y directions to create a 67×67 square grid of ~100×100 μm^2 in size. In addition, the height of the stage was adjusted to account for any slight tilting of the samples so that at each point on the grid the excitation spot was the same size.

The light emitted by the sample was collected by an optic fibre and directed into a spectrometer (Ocean Optics, QE65000) after passing through a long pass filter to eliminate scattered light from the source. An emission spectrum was taken at each point and its coordinates were recorded. The laser fluence was varied with a neutral density (ND) filter wheel and measured by a power meter to produce three maps over the same area on each sample, one at each of three different excitation powers, corresponding to excitation densities of: 12, 41 and 130 μJ cm^{-2} $pulse^{-1}$. These excitation densities were chosen to correspond to the three distinct regions of a typical efficiency droop curve [16]: the initial rise in efficiency with

increasing excitation power at low powers, the plateau region where the curve begins to flatten off, and the droop in efficiency at high excitation densities.

The variation in the behaviour of the power-dependent PL properties between areas of high and low emission intensity was also investigated. To identify regions of high and low brightness within the area mapped, the spectrally-integrated PL intensity was calculated from the spectra obtained at each point. The stage was then moved back to the x, y and z coordinates recorded for points corresponding to the identified bright and dim regions. Power-dependent PL spectra were obtained using the same setup and a ND filter wheel was used to vary the excitation power between 9 and 245 μJ cm^{-2} pulse^{-1} (which, using an absorption coefficient of 3×10^4 cm^{-1} [17], correspond to estimated carrier densities ranging from 1.6×10^{11} to 4.3×10^{12} carriers cm^{-2} QW^{-1} pulse^{-1}). In this way, power-dependent PL spectra extending into the efficiency droop regime were measured at points corresponding to a bright and a dark region on each sample.

3. Results & Discussion

The micro-PL maps reveal spatial variation on the order of 10s of μm in the emission across both the green and blue-emitting samples. In Figure 1, maps of spectrally-integrated intensity, normalised to the average value, across sample B730 taken at low (a) and at high (b) excitation power densities show that this intensity variation decreases as excitation power is increased. This effect is more noticeable for sample G706: comparison of the low (e) and high (f) power intensity maps show that the variation seen at low power almost completely disappears when the power is increased, except for in a small area in the lower right corner of both maps. The maps of the peak emission energy and bandwidth taken at low power across the blue (c & d) and green (g & h) samples show clear correlation to the patterns of variation seen in the corresponding intensity maps. The maps for both samples show that regions of higher energy emission correspond to regions of broader linewidth. The correlation between peak energy and integrated intensity, however, is opposite in the two samples: in B730 the correlation is negative, while in G706 the correlation is positive. The reason for this difference in behaviour between green and blue samples is not yet established and is the subject of further investigation.

In order to investigate the effect of this spatial variation on droop measurements, the dependence of emission efficiency (i.e. spectrally-integrated intensity normalised by carrier density) on carrier density was obtained in both a bright and dark region on each sample, as shown in Figure 2. For B730, the difference in efficiency between the bright and dark regions decreases steadily from 25% to 10% as the carrier density increases from 1.6×10^{11} to 4.3×10^{12} carriers cm^{-2} QW^{-1} pulse^{-1}. However, for G706 the efficiency difference is about 20% initially, but disappears by the time the carrier density reaches 2×10^{12} carriers cm^{-2} QW^{-1} pulse^{-1}. For both samples, the onset of droop in the dark patches occurs at a higher carrier density than in the bright. For B730, the curve corresponding to a dark region begins to droop at a carrier density $\sim 1.2 \times$ higher than the curve for the bright region, while for G706 the difference is larger, with the onset of droop differing by a factor of 1.8 between bright and dark regions.

One possible explanation for this behaviour is that there is a higher density of extended defects in the dark regions. In [18], Schubert et al suggest that InGaN/GaN LEDs with high dislocation densities have a lower peak efficiency but shallower droop than those with lower dislocation densities. They propose that higher dislocation densities correspond to a decrease in non-radiative recombination lifetime at low currents, leading to a reduced carrier density [18]. The dark regions on our maps could therefore correspond to regions of higher dislocation density. The convergence of the integrated intensity curves in the droop regime could then be due to a shallower droop and lower peak in the dark regions.
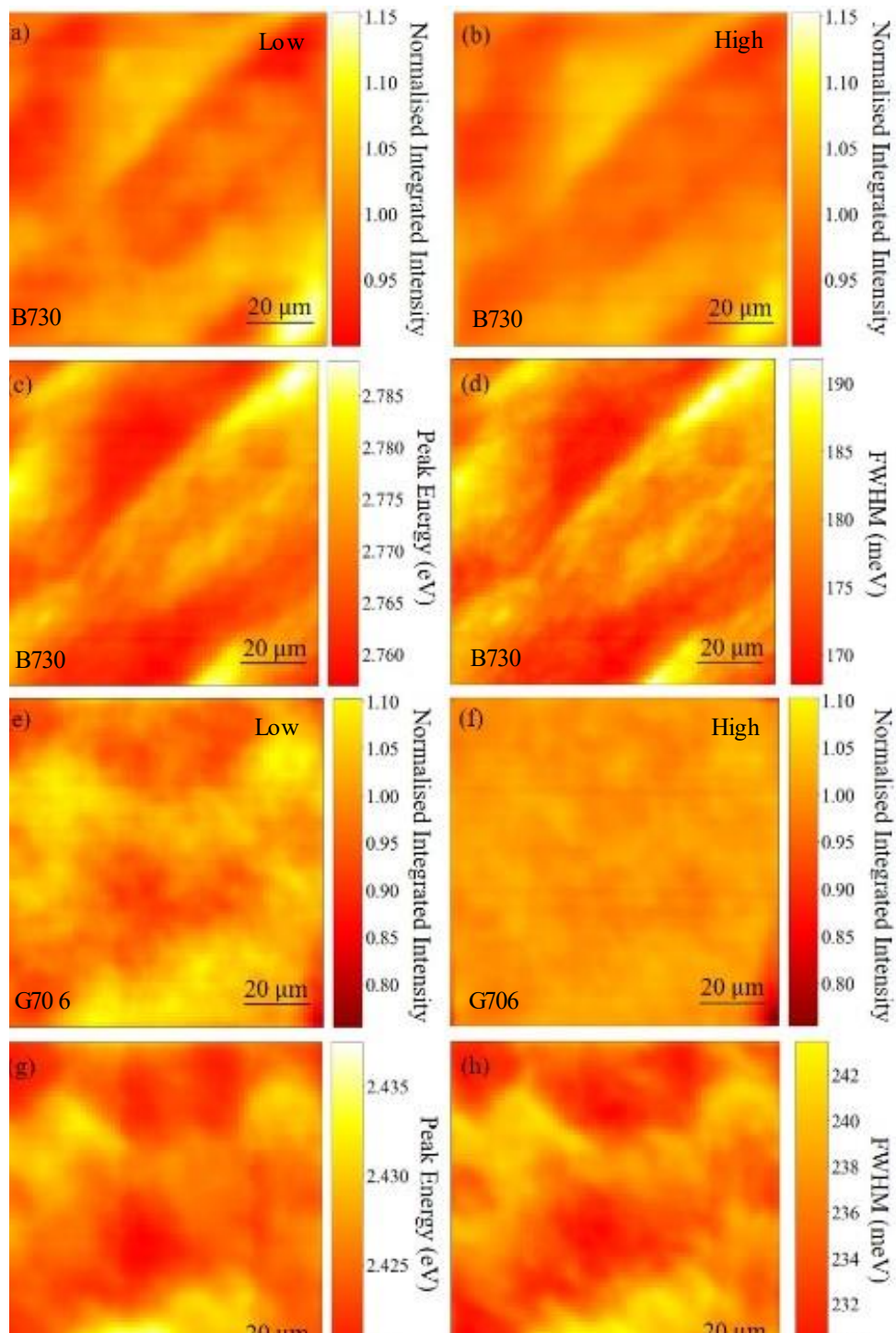
Figure 1 – Micro-PL maps of intensity, peak energy and FWHM for the blue (a to d) and green (e to h) samples. The change in the intensity maps between high (a & e) and low (b & f) power densities is also shown for both samples.

It is also possible that spatial variation comes from regions of differing well width fluctuation (WWF) density. Oliver et al show in [14] that InGaN/GaN multiple QWs exhibit higher peak electroluminesence efficiencies when WWFs are present, possibly because the activation energy for defect-related non-radiative recombination is higher for carriers localised at WWFs. They [14] also show that the peak intensity occurs at lower carrier densities if WWFs are present and that the IQE curves from samples with and without WWFs begin to

converge at high current densities. The bright regions in our maps could therefore correspond to regions of increased WWF density.
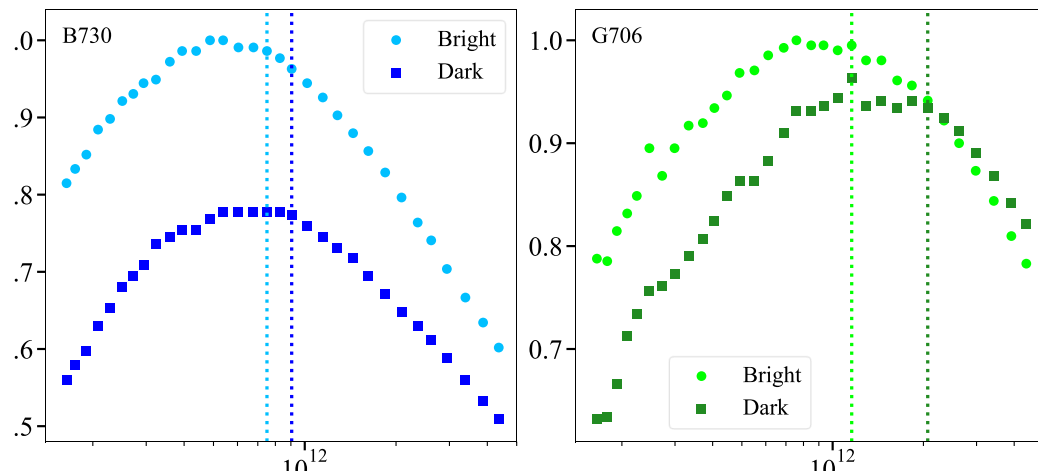

Figure 2 - Excitation power dependence of integrated PL intensity, in bright and dark spots on samples B730 (left) and G706 (right). The curves are normalised to the maximum value in each bright region. The vertical dotted lines indicate the onset of droop.

To quantify the extent by which photoluminescence measurements taken at different positions across the samples could vary for different collection areas, the maximum variation in peak emission energy and spectrally-integrated intensity between any two positions is investigated. This was done by finding the largest difference between any two points on the peak energy and integrated intensity graphs when averaging over different sized areas, corresponding to different collection spot sizes. The results are shown in Figure 3 for low, high and medium excitation powers of 12, 41 and 130 µJ cm^{-2} pulse^{-1}.
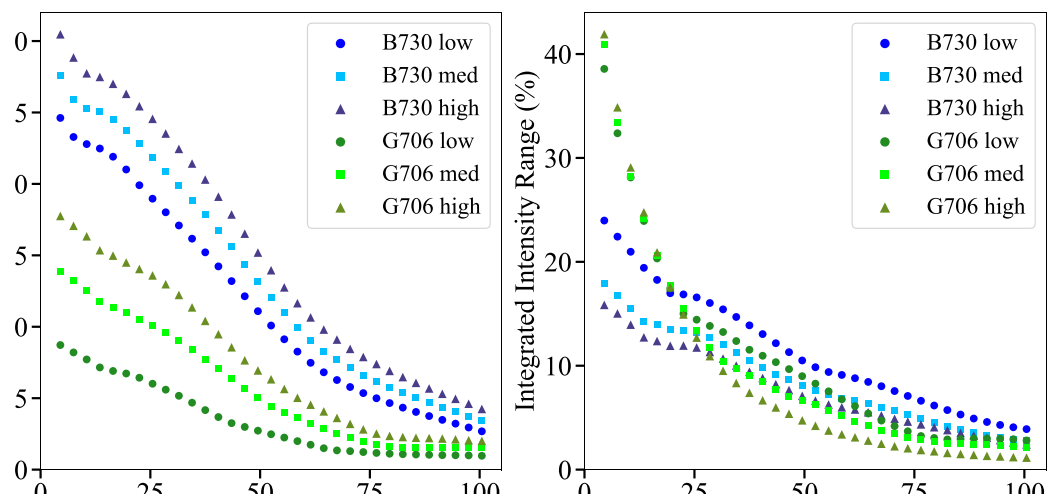

Figure 3 - The maximum difference in peak energy (left) and intensity (right) measured at each excitation power between different positions on the µPL maps when averaging over varying detection spot sizes.

For both samples, the maximum variation in peak energy increases with increasing excitation power and decreases with increasing collection spot size. With a collection spot size of 4 µm, the maximum variation in peak energy is between 25 meV and 30 meV for B730 and between 9 meV and 18 meV for G706. The maximum variation in integrated intensity similarly decreases with increasing collection spot size, but also decreases with increasing excitation power. For spot sizes less than 25 µm, the curves for G706 deviate from this trend

and converge due to the persistent presence of the dark region shown in the lower right corner of Figures 1e & 1f. The maximum variation in intensity with a collection spot size of 4 μm is between 16 % and 24 % in B730 and 40 % in G706. The variation drops below ∼ 10 % for detection spot sizes greater than 50 μm at all excitation levels.

To investigate how the spread of variation in intensity between any two positions across each sample compares to the maximum variation, boxplots indicating the interquartile ranges when averaging over spot sizes of 4 μm and 50 μm are shown in Figure 4. The 99th percentiles are indicated by horizontal lines, with points outside this range in red.
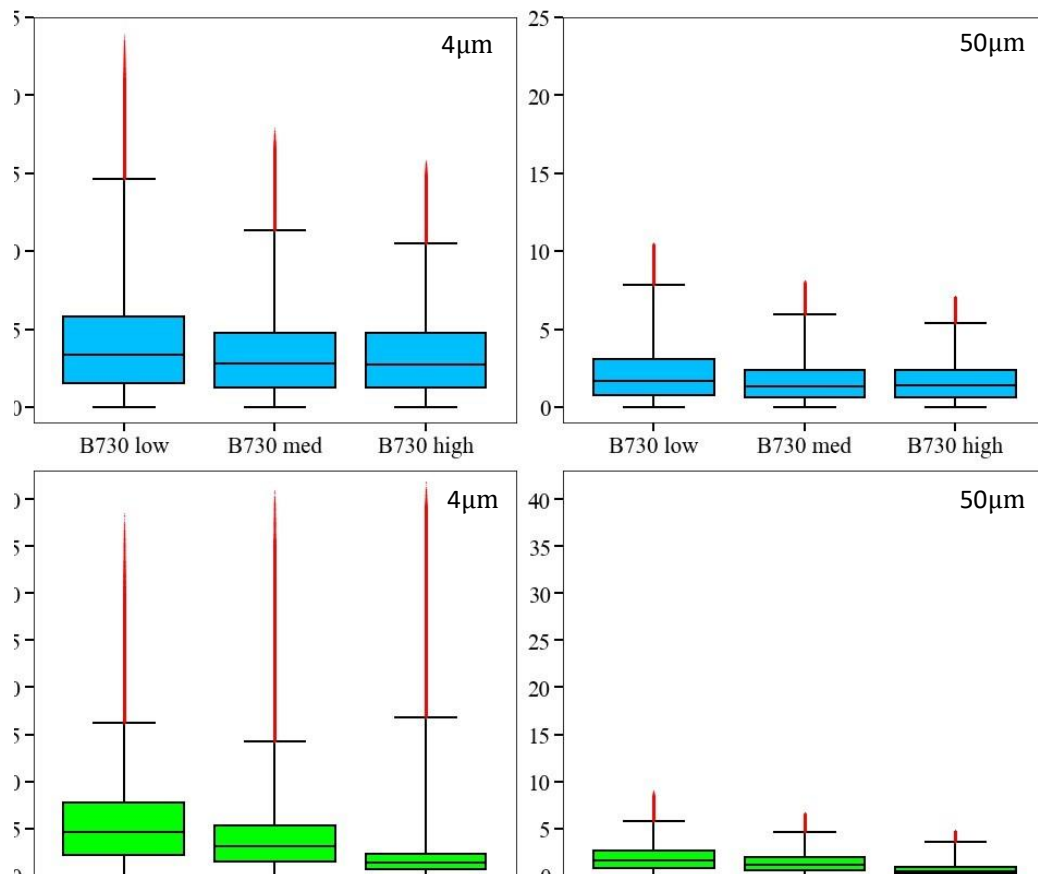

Figure 4 – Boxplots showing the interquartile ranges (boxes), medians (horizontal lines within boxes) and ranges (vertical lines) of intensity variation for B730 (top) and G706 (bottom) when averaging over spot sizes of 4 μm and 50 μm. The 99th percentiles are indicated by horizontal lines, with points outside this range in red.

In B730, the 99th percentile, while up to 10% below the maximum variation, follows the same trend as in Figure 3 – decreasing with increasing excitation power – for both spot sizes. The upper quartile, however, drops between low and medium power, but then remains constant. In G706, both the upper quartile and 99th percentile decrease as excitation power increases for a 50 μm spot size, while for 4 μm, only the upper quartile shows this trend. The outliers extend much further (∼ 25%) beyond the 99th percentile for the smaller spot size in G706 than in B730, while the extension is similar in both samples (∼ 2%) for the larger spot size. This suggests that the dark feature in the lower right corner of Figures 1e & 1f effects the maximum intensity variation much more for smaller spot sizes, perhaps explaining the deviation below 25 μm of G706 in Figure 3 from the trend of decreasing variation with increasing detection spot size.

4. Summary & Conclusions

Micro-PL maps show spatial variation on length scales of ~10s of μm in the integrated intensity, peak emission energy and FWHM across green and blue-emitting InGaN/GaN QW samples. The spatial variation in PL intensity decreases as excitation power density is increased. The maximum difference in measured intensity between any two positions on the maps decreases as collection spot size increases such that the variation only falls below ~ 10% at all excitation densities for a spot size of more than 50 μm. For a spot size of 4 μm, the 99th percentile of intensity variation is less than 20%, but even within the randomly selected 100×100 μm^2 area, there were some outlier points that corresponded to 40% variation. If a small collection spot is used, then this variation within samples could be an important consideration when comparing PL measurements taken on different samples, especially if such measurements differ by less than ~ 40 %.

Excitation power dependent PL shows that the conversion efficiencies measured in bright and dark regions begin to converge as excited carrier density increases into the droop regime, but that the onset of droop can occur at an excited carrier density 1.8 × higher in dark regions than in bright. It may therefore be the case that the size of the detection spot used in droop measurements should be an important consideration if reproducible results are to be obtained.

References

[1]   Christian G M, Schulz S, Kappers M J, Humphreys C J, Oliver R A and Dawson P 2018 Recombination from polar InGaN/GaN quantum well structures at high excitation carrier densities *Physical Review B* **98** 1–9

[2]   Iveland J, Martinelli L, Peretti J, Speck J S and Weisbuch C 2013 Direct measurement of auger electrons emitted from a semiconductor light-emitting diode under electrical injection: Identification of the dominant mechanism for efficiency droop *Physical Review Letters* **110** 1–5

[3]   David A, Young N G, Hurni C A and Craven M D 2019 Quantum Efficiency of III-Nitride Emitters: Evidence for Defect-Assisted Nonradiative Recombination and its Effect on the Green Gap *Physical Review Applied* **11** 1

[4]   Dai Q, Schubert M F, Kim M H, Kim J K, Schubert E F, Koleske D D, Crawford M H, Lee S R, Fischer A J, Thaler G and Banas M A 2009 Internal quantum efficiency and nonradiative recombination coefficient of GaInN/GaN multiple quantum wells with different dislocation densities *Applied Physics Letters* **94** 1–4

[5]   Verzellesi G, Saguatti D, Meneghini M, Bertazzi F, Goano M, Meneghesso G and Zanoni E 2013 Efficiency droop in InGaN/GaN blue light-emitting diodes: Physical mechanisms and remedies *Journal of Applied Physics* **114**

[6]   Davies M J, Dawson P, Hammersley S, Zhu T, Kappers M J, Humphreys C J and Oliver R A 2016 Comparative studies of efficiency droop in polar and non-polar InGaN quantum wells *Applied Physics Letters* **108** 252101

[7]   Shahmohammadi M, Liu W, Rossbach G, Lahourcade L, Dussaigne A, Bougerol C, Butté R, Grandjean N, Deveaud B and Jacopin G 2017 Enhancement of Auger recombination induced by carrier localization in InGaN/GaN quantum wells *Physical Review B* **95** 1–10

[8]   Jeong M S, Kim J Y, Kim Y W, White J O, Suh E K, Hong C H and Lee H J 2001 Spatially resolved photoluminescence in Ingan/gan quantum wells by near-field scanning optical microscopy *Applied Physics Letters* **79** 976–8

[9]   Jeong M S, Kim Y W, White J O, Suh E K, Cheong M G, Kim C S, Hong C H and Lee H J 2001 Spatial variation of photoluminescence and related defects in InGaN/GaN quantum wells *Applied Physics Letters* **79** 3440–2

[10]   Okamoto K, Kaneta A, Kawakami Y, Fujita S, Choi J, Terazima M and Mukai T 2005 Confocal microphotoluminescence of InGaN-based light-emitting diodes *Journal of Applied Physics* **98**

[11]   Okamoto K, Choi J, Kawakami Y, Terazima M, Mukai T and Fujita S 2004 Submicron-Scale Photoluminescence of InGaN/GaN Probed by Confocal Scanning Laser Microscopy

Japanese Journal of Applied Physics, Part 1: Regular Papers and Short Notes and Review Papers **43** 839–40

[12]   Yim S Y, Kim J H, Jeong M S, Park S H and Lee J 2011 Power dependent micro-photoluminescence of green-InGaN/GaN multiple quantum wells *Japanese Journal of Applied Physics* **50**

[13]   Hammersley S, Kappers M J, Massabuau F C P, Sahonta S L, Dawson P, Oliver R A and Humphreys C J 2015 Effects of quantum well growth temperature on the recombination efficiency of InGaN/GaN multiple quantum wells that emit in the green and blue spectral regions *Applied Physics Letters* **107** 132106 1-6

[14]   Oliver R A, Massabuau F C P, Kappers M J, Phillips W A, Thrush E J, Tartan C C, Blenkhorn W E, Badcock T J, Dawson P, Hopkins M A, Allsopp D W E and Humphreys C J 2013 The impact of gross well width fluctuations on the efficiency of GaN-based light emitting diodes *Applied Physics Letters* **103** 141114 1-4

[15]   Alanis J A, Saxena D, Mokkapati S, Jiang N, Peng K, Tang X, Fu L, Tan H H, Jagadish C and Parkinson P 2017 Large-scale statistics for threshold optimization of optically pumped nanowire lasers *Nano Letters* **17** 4860–5

[16]   Shen Y C, Mueller G O, Watanabe S, Gardner N F, Munkholm A and Krames M R 2007 Auger recombination in InGaN measured by photoluminescence *Applied Physics Letters* **91** 1411011 1-3

[17]   Ambacher O, Brunner D, Dimitrov R, Stutzmann M, Sohmer A, Scholz F 1998 Absorption of InGaN single quantum wells determined by photothermal deflection spectroscopy *Japanese Journal of Applied Physics* **37** 745-752

[18]   Schubert M F, Chhajed S, Kim J K, Schubert E F, Koleske D D, Crawford M H, Lee S R, Fischer A J, Thaler G, Banas M A 2007 Effect of dislocation density on efficiency droop in GaInNGaN light-emitting diodes *Applied Physics Letters* **91** 23 231114